Biophysical Journal, Volume *112*

Supplemental Information

Signal Destruction Tunes the Zone of Activation in Spatially Distributed Signaling Networks

Kalinga Pavan Silva, Prithiviraj Chellamuthu, and James Q. Boedicker

Plasmids

Plasmids to create the sender and interferer were obtained from Addgene. The plasmids were inserted into *E. coli Dh5alpha.* The plasmids in the sender and interferer were based on study (1).

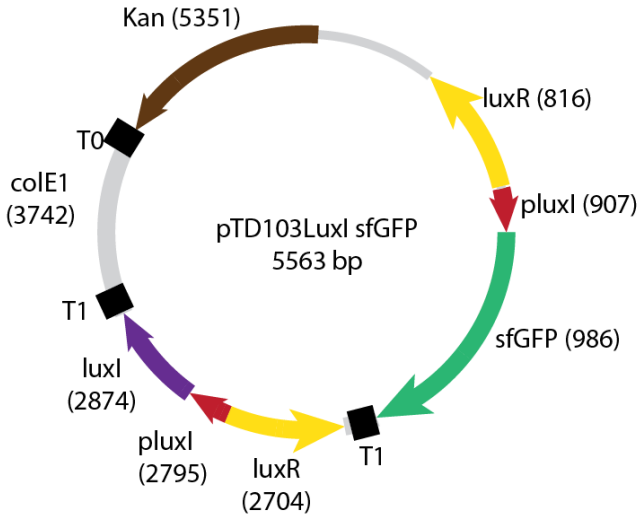

Figure S1: The map for the plasmid in the sender. *luxI* encodes for the production of the AHL 3-oxo-c6-HSL. *luxR* encodes for the production of the receptor protein LuxR. Once the AHL binds to the LuxR protein it could bind to the *pluxI* promoter and activate the expression of the genes *luxI*, *luxR* and *sfGFP*.

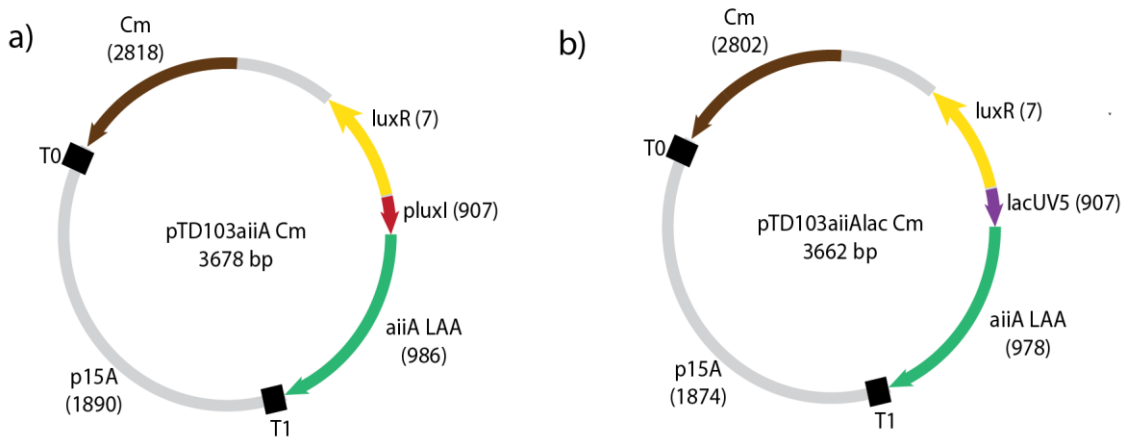

Figure S2: The map for the plasmid in the Interferer (a). regulated under the *pluxI* promoter (b). constitutive under the *lacUV5* promoter. For the regulated interferer strain, the AHLs diffusing from the sender will bind to the LuxR protein, and activate the *pluxI* promoter and express the *aiiA* gene while for the constitutive interferer strain the *aiiA* gene will be produced constitutively. The *aiiA* gene will encode for the production of the degradative enzyme AiiA.

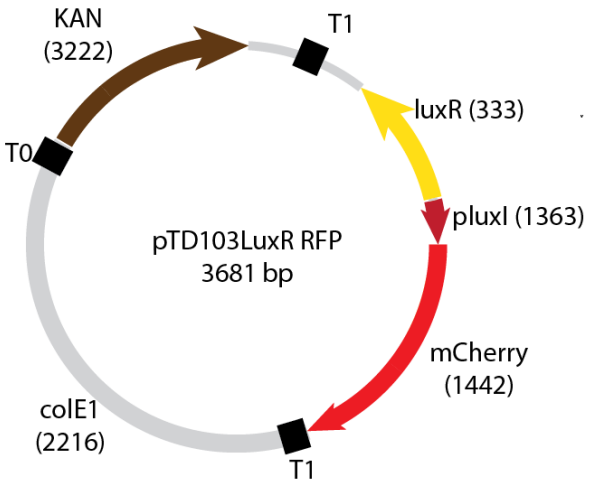

Figure S3: The map for the plasmid in the receiver. The *pluxI* promoter will activate due to the diffusing AHLs from the sender. Once activated, LuxR and the mCherry fluorescent protein will be produced. We constructed the receiver, based on the ptD103 plasmid. The *luxI* and *sfGFP* genes were deleted from the ptD103luxI sfGFP plasmid and the *mCherry* sequence was added in place of the *sfGFP* gene.

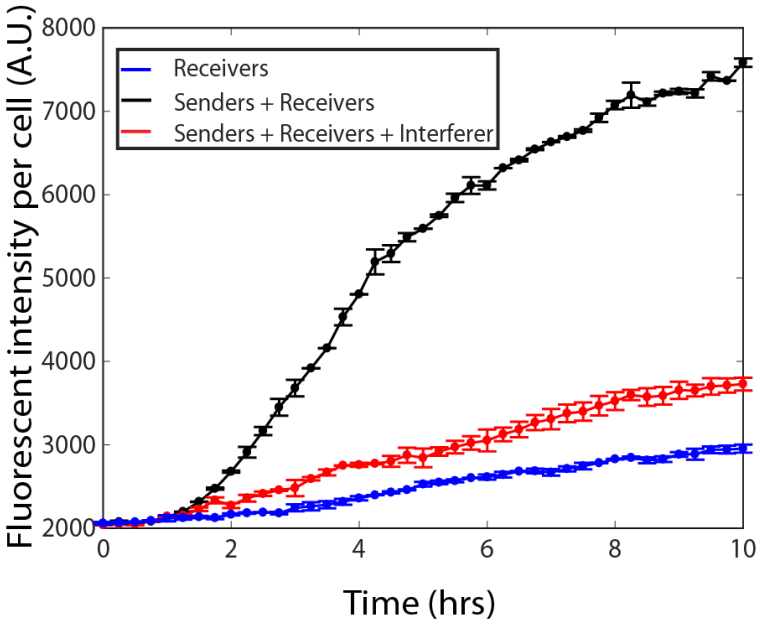

Figure S4: The change in fluorescent intensity per cell of the receivers as a result of coculture with the sender strain or the sender strain and the interferer strain. Fluorescent intensity was measured in the plate reader at 37 °C as described in the main text.

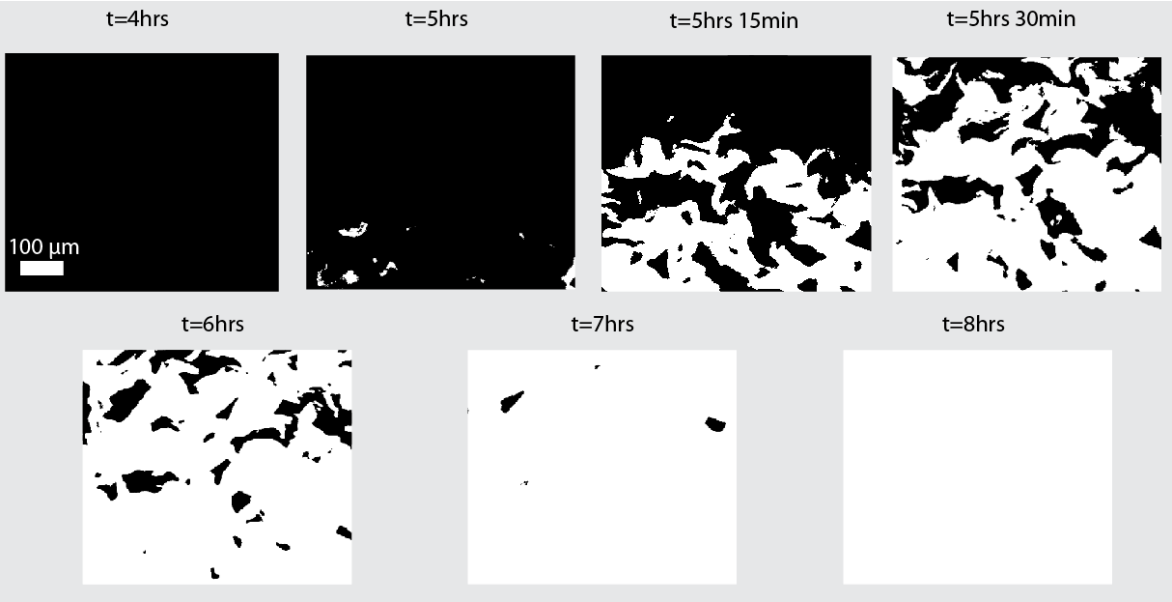

Figure S5: Analysis of growth of the artivation for the case of no interference. At the threshold (10% of the maximal pixel value for the microscope), we see clear activation (white) of the receivers at a distance of 2 mm (bottom edge of the frame) from the senders. The images here are taken from the microscope and the size of each frame is 750 µm. The receiver activates from bottom to top.

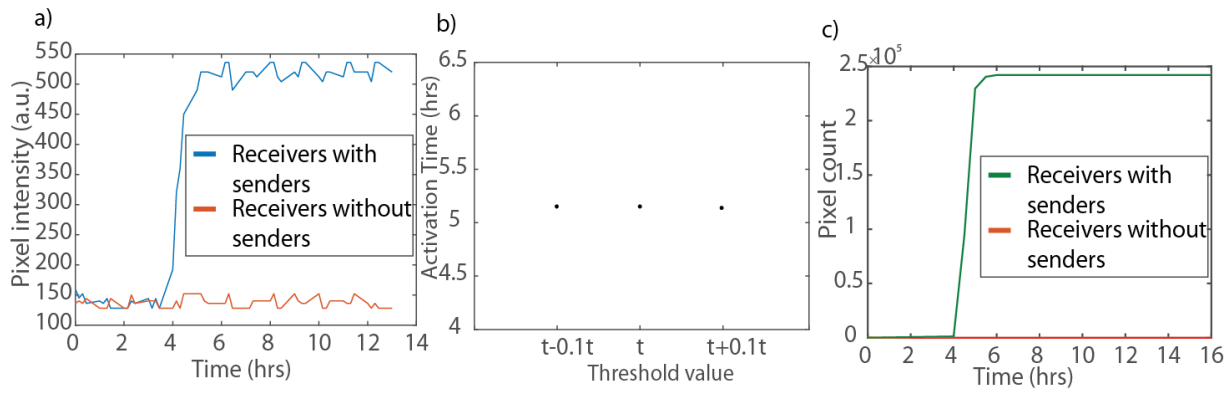

Figure S6: Sensitivity of results to the activation threshold value. a) The pixel intensity of the receivers over time at a distance 2 mm from the sender and in a negative control of receivers without added sender. b) The calculated activation times when we change the threshold was raised or lowered by 10%. c) Upon applying the threshold, the number of pixels above threshold was counted for receiver cells 2 mm from the sender and in the no sender negative control.

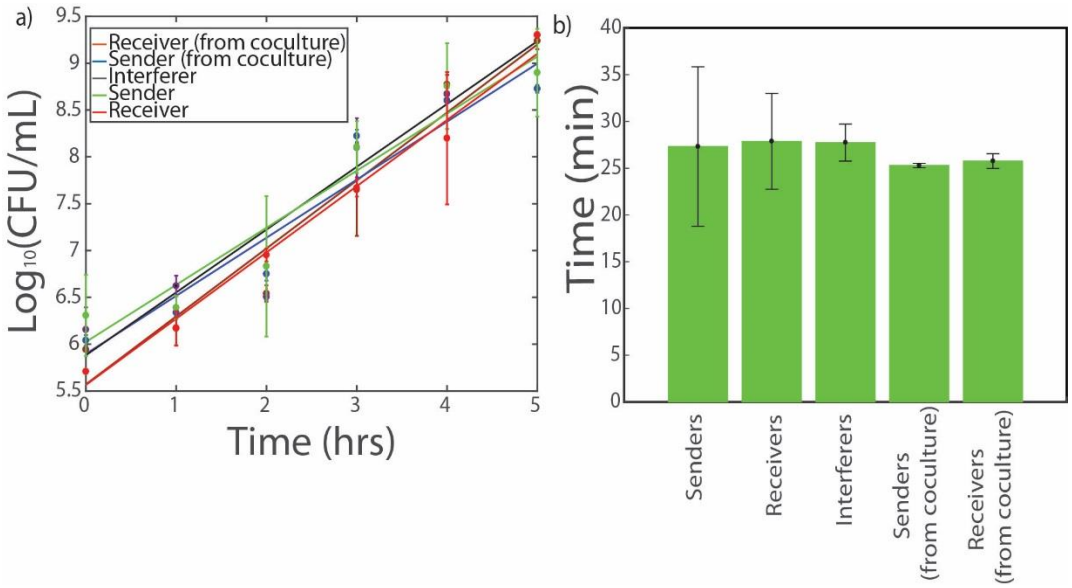

Figure S7: Addition of the interferer strain did not significantly change the doubling time of the sender or the receiver. a) Growth curves for the sender, receiver, and interferer strain alone and in coculture. In coculture experiments, selective plating enabling tracking of individual species. b). Fits to the linear doubling times of the sender, receiver, and interference strains. The errorbars show standard deviation from four replicates. A standard unpaired t test was used to calculate the two tailed p value. Comparisons between the doubling times of the senders or receivers with and without addition of the interferer had $p > 0.5$.

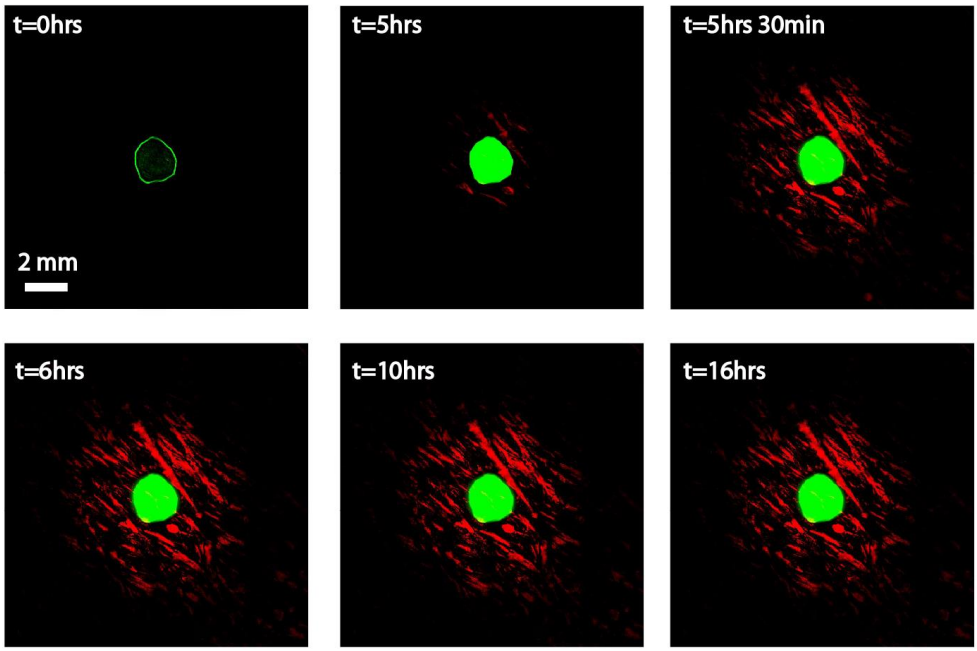

Figure S8: The plate assay experiment shown here for normalized interference level 0.9 shows that the activation of the receivers stop at a distance 2.3 mm. The experiments were done for 16 hours, and no propagation in the activation was observed. The dark areas within activated regions are the result of variability in the initial distribution of receiver cells

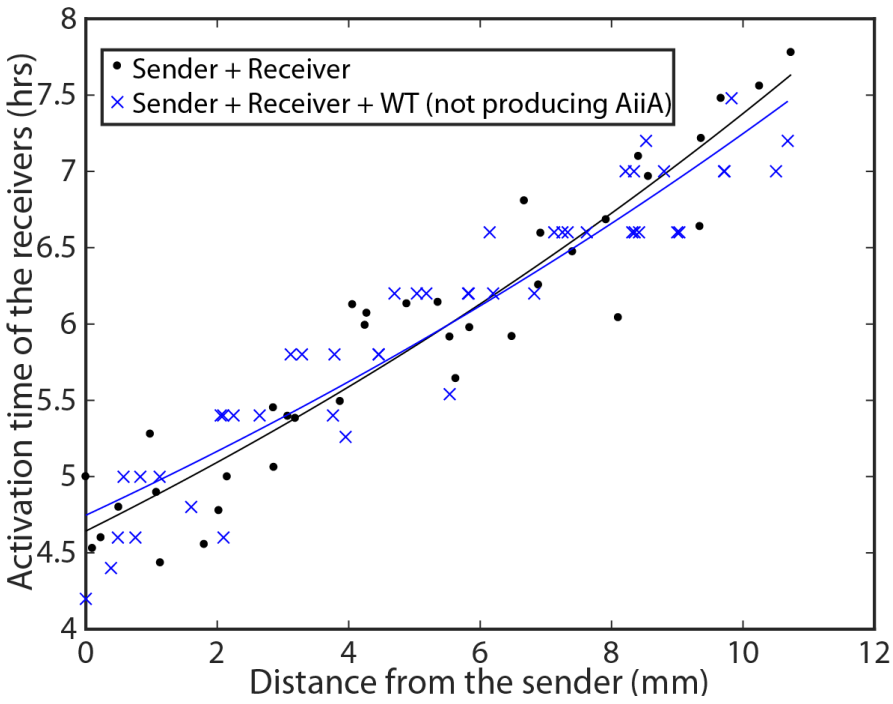

Figure S9: Control experiment compares the activation dynamics of the sender and receiver alone (black dots) or when paired with the wild type (WT) host that does not produce the AiiA enzymes (blue X's). Plate-assay setup as described in the main text.

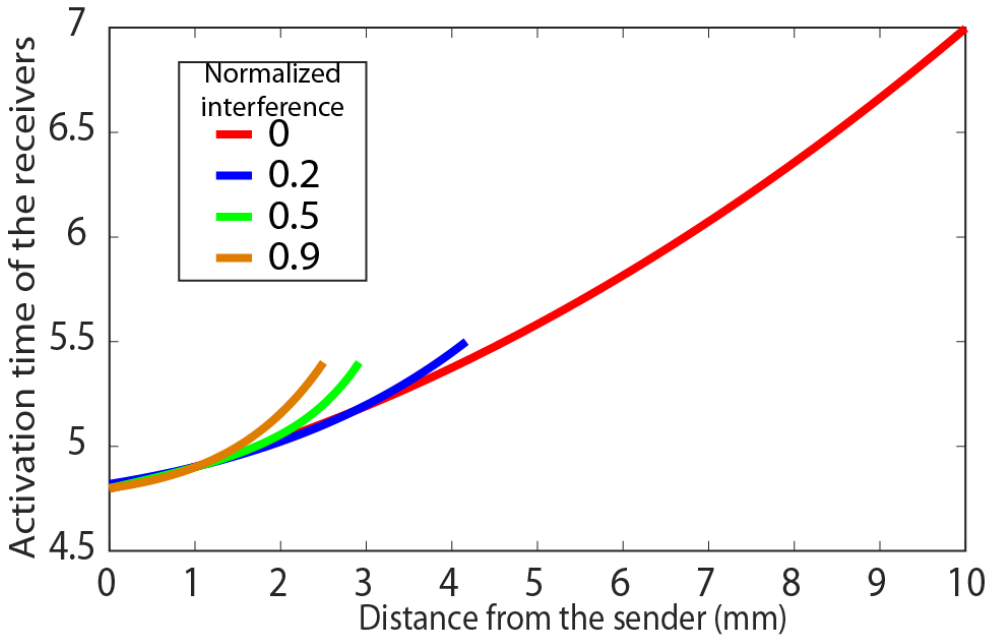

Figure S10: Simulation results for the activation time vs. distance for the receivers

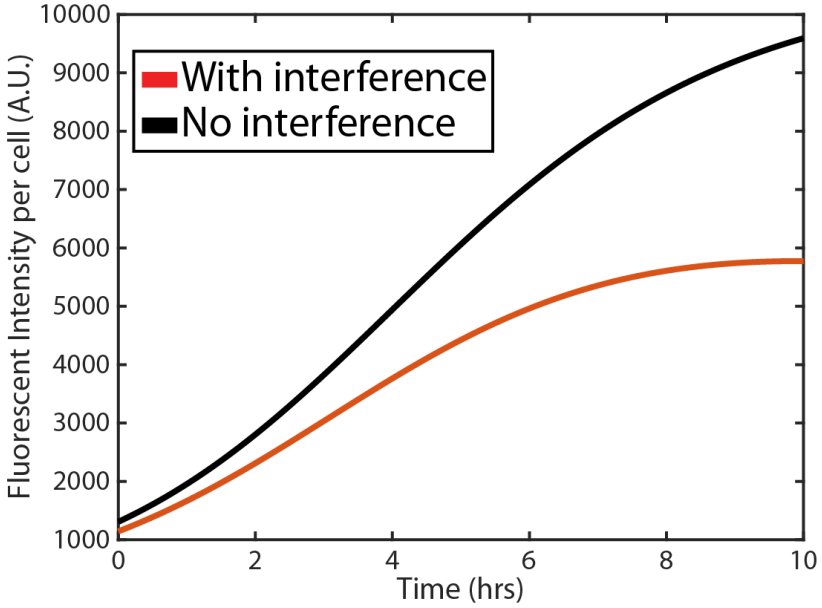

Figure S11: The model predictions made for the changes in the fluorescent intensity per receiver cell, with and without the AiiA species. Here we obtain the concentration profiles of the AHLs in a well-mixed setup and convert it to the fluorescent intensity per cell by multiplying with an arbitrary value.

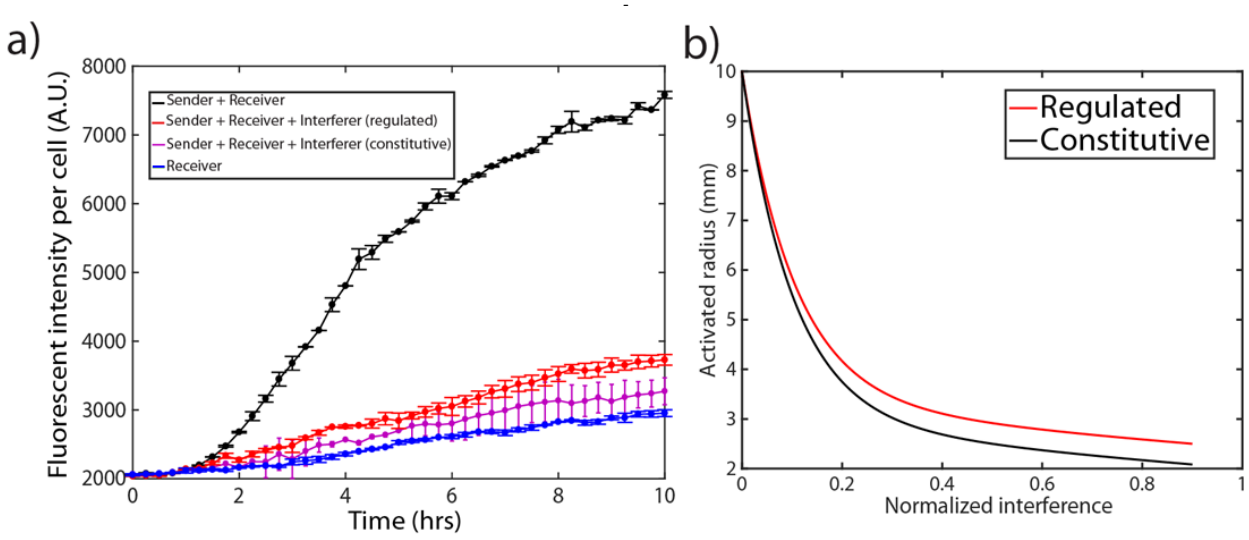

Figure S12: Regulated vs constitutive production of AiiA in the interference strain. (a). Plate reader experiments shows that the constitutive interferer (purple) yields a similar response to the regulated interferer (red). (b). Simulations confirms that the plate assay setup will yield a similar response to the regulated case. To simulate the constitutive production of AiiA, we delete the Hill's coefficient appearing in equation {3} such that the AiiA strain will constitutively produce the AiiA at a constant rate of production of 2.3×10^{-9} nM hrs^{-1} per cell.

Calculation of the number of proteins per cell for the production rate of AiiA

In this section we will justify that the production rate assumed for AiiA (2.3×10^{-10} nmol hrs^{-1} per cell) in the modelling is reasonable. The system is simulated for 10 hours.

At t=10 hours, the amount of AiiA per cell can be estimated as: 2.3×10^{-10} nmol hrs^{-1} per cell x 10 hours= 2.3×10^{-9} nmol per cell or 2.3×10^{-18} mol per cell.

In molecules, AiiA per cell would be: 2.3×10^{-18} mol per cell x 6.022×10^{23} molecules/mol ~ 10^{6} molecules per cell.

Hence, we estimate on the order of 10^{6} AiiA proteins produced per cell at t=10 hours in the simulations, which is within the range of the standard number of proteins per bacterial cell (2), particularly for a production from a gene encoded on a plasmid.

Calculating the fluorescence in a mixed culture using the plate reader

In this section our objective is to calculate the fluorescence of a species in a mixed culture. In the mixed culture, there will be two species, one with a particular fluorescence (ex: RFP) and the other strain will not have the same fluorescence. We experimentally measure the total fluorescence of the mixture using a plate-reader.

We define the following terms,

Fluorescence readout from the plate reader = Fl;

Number of cells = n;

Optical density readout from the plate reader = O;

Background fluorescence per cell= α;

Fluorescence per protein = ω;

Number of fluorescent protein per cell = f;

Absorbance of light per cell = β;

Let's consider a general case where species A produces the fluorescence (ex:RFP) and species B doesn't produce any or the same fluorescence as species A. There will be a background fluorescence due to the light scattering off the edges of the cell.

First we will consider the total fluorescence of the mixed culture;

$Fl_{total} = n_A f \omega + n_A \alpha_A + n_B \alpha_B + Fl_m$ **{4}**

Where, Fl_m is the background fluorescence of the media.

The corresponding optical density will be;

$O_{total} = n_A \beta + n_B \beta + O_m$ **{5}**

Where, O_m is the background fluorescence of the media.

If species B is grown in a single culture the fluorescence of species B will be;

$Fl_B = n_B \alpha_B + Fl_m$ **{6}**

The corresponding optical density of species B will be;

$O_B = n_B \beta + O_m$ **{7}**

Since we use E. *coli* (DH5alpha, NEB10beta) cells for all of the different species in our study, we assume that the background fluorescence per cell in all the cells is the same. ($\alpha_A = \alpha_B = \alpha_1$)

Now, the total fluorescence of the mixed culture for all the cells,

$$\frac{Fl_{total} - Fl_m}{O_{total} - O_m} = \frac{n_A f \omega + n_A \alpha_1 + n_B \alpha_1}{n_A \beta + n_B \beta} \quad \textbf{\{8\}}$$

The total fluorescence of species B in the single culture,

$$\frac{Fl_B - Fl_m}{O_B - O_m} = \frac{n_B \alpha_1}{n_B \beta} \quad \textbf{\{9\}}$$

Now lets define Δ_A ={8} - {9}

$$\Delta_A = \frac{n_A f \omega + n_A \alpha_1 + n_B \alpha_1}{n_A \beta + n_B \beta} - \frac{\alpha_1}{\beta}$$

$$= \frac{n_A\, f\, \omega + n_A\, \alpha_1 + n_B\, \alpha_1 - (n_A + n_B)\alpha_1}{(n_A + n_B)\, \beta}$$

$$= \frac{n_A\, f\, \omega}{(n_A + n_B)\beta} \qquad \textbf{\{10\}}$$

Now from **{5};**

$$(n_A + n_B)\beta = O_{total} - O_m \qquad \textbf{\{11\}}$$

$\emptyset_A = n_A\, f\, \omega$, is the total fluorescence of the species A in the mixture.

Hence by using {10} and {11},

$$\emptyset_A = (\Delta_A)\,(O_{total} - O_m) \qquad \textbf{\{12\}}$$

Hence, by taking the fluorescent readout (F) and the optical density readout (O) of the mixed sample and the single cultured B sample we can calculate the total fluorescence of the species A in the mixture.

Finally we deduce the total fluorescence per cell $= \frac{\emptyset_A}{(O_{total} - O_m)}$ **{13}**

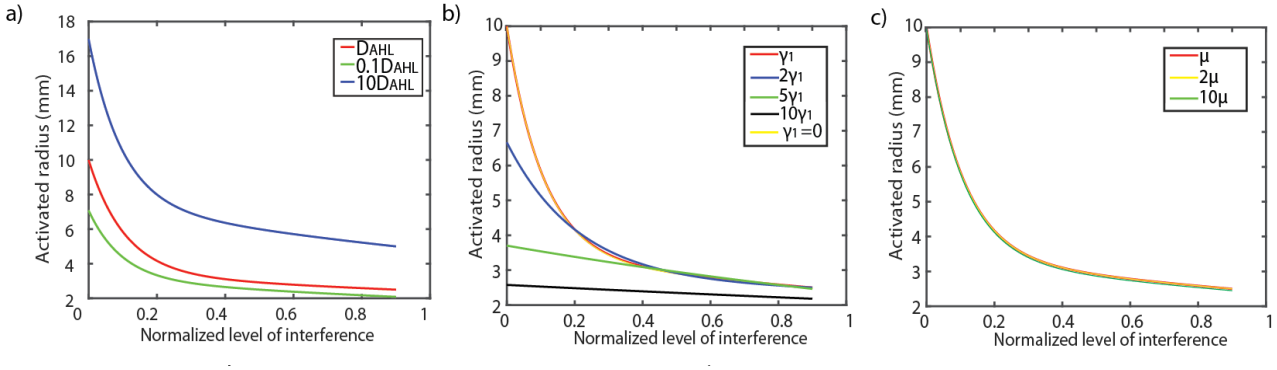

Figure S13: To understand the parameters that dictate the dynamics of the activation zone we changed (a) the sender AHL diffusion coefficient (b) the sender AHL degradation rate by the media (γ_1). In our experiment these values are constants. It can be seen that the degradation by the media is not a major contributor to the inhibition zone since even at zero degradation (γ_1 =0, yellow line), we see no deviations from γ_1 (red line). If the AHLs are degraded by the media at a higher rate, the activation radius for lower normalized interference values decreases, but above a certain γ_1 value, the radius for higher normalized interference seems to be affected as well. This is due to effect from γ_1 being comparable to the effect from the interferer. Additionally, we changed (c) the growth rate of the signal sender and observed no shift in the plot. This is due to the fact that the senders are already active when they are loaded into the plate such that levels of activation and degradation change proportionally.

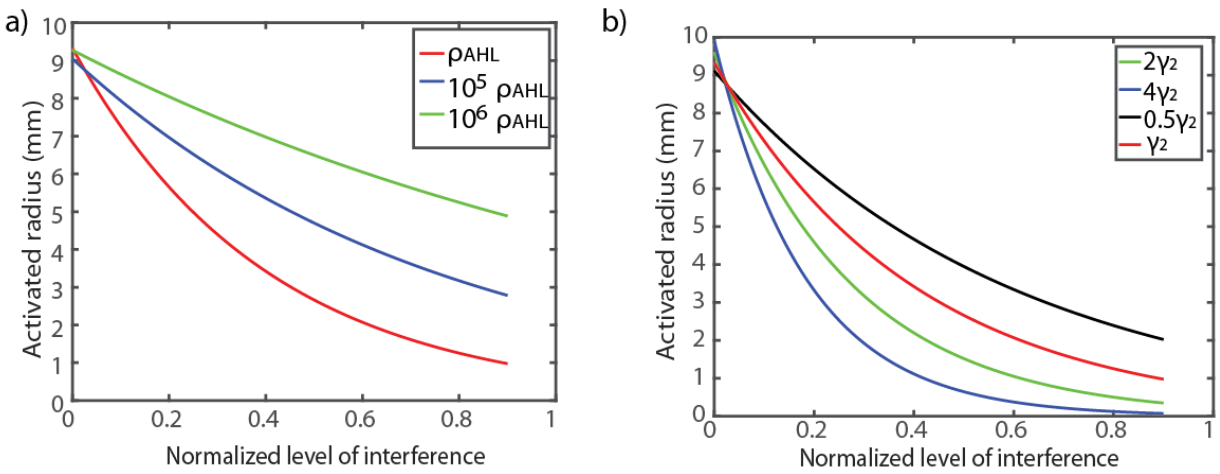

Figure S14: In simulations changing (a) the production rate of the AHL, (b) the degradation rate of the AHLs by the interferers. Compared to known quorum sensing production rates, the production rates used here are very large to have any significant effect on the plot. The plot is more sensitive towards the degradation rate of the interferers on the other hand, as seen in (b), doubling or halving the degradation rate shifts the plot significantly.

Testing the model for effects of the growth interactions, diffusion coefficients, degradation rates and internalization of the signal

To test the possible effect of growth influences on the sender-receiver system caused by the interferer we considered a competitive Lotka–Volterra equation (3),

$$\frac{\partial n}{\partial t} = \mu\, n\left(1 - \frac{n_{Total}}{s}\right) - \alpha_1\, n\, n_{interferer} \qquad \textbf{\{14\}}$$

where, α_1 is the growth effect the interfering species has on the sender-receiver system.

To test the effect of signal internalization we modified equation **{3}** such that,

$$\frac{\partial [AHL]}{\partial t} = D_{AHL}\nabla^2[AHL] + n_{AHL}\left(\rho_{AHL}\frac{[AHL]^{m_1}}{[AHL]^{m_1} + {\theta_1}^{m_1}} + \rho_{b1}\right) - \gamma_1[AHL] - \alpha_2\, n_{interferer}\frac{[AHL]^{m_4}}{[AHL]^{m_4} + {\theta_4}^{m_4}} \qquad \textbf{\{15\}}$$

where, α_2 is the AHL internalizing rate per interfering cell which is modulated by the number of AHLs present in the vicinity of the interferer.

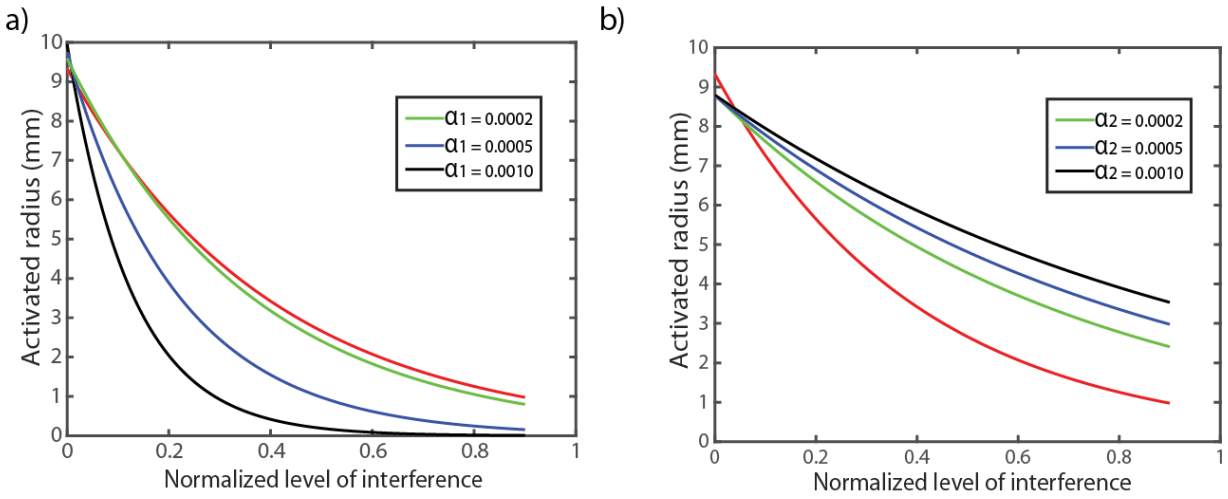

Figure S15: Change in activation dynamics as a result of growth interactions between species (a) or AHL internalization (b). To simulate these conditions, we used equations **{14} and {15}.** For both conditions, we assume that there is no AHL degradation by the interference strain, the influence of the interferer on the receiver is solely due to either growth influences or AHL internalization. The red curve represent the usual case when the interferer degrades the AHL, plotted here for comparison. For (b) we used, m_4 = 2.5 and $\theta_4 = 70\ nM$.

.

Supplemental References:

1. **Danino T**, **Mondragón-Palomino O**, **Tsimring L**, **Hasty J**. 2010. A synchronized quorum of genetic clocks. Nature **463**:326–330.

2. **Milo R**. 2013. What is the total number of protein molecules per cell volume? A call to rethink some published values. Bioessays **35**:1050–1055.

3. **Bomze IM**. 1995. Lotka-Volterra equation and replicator dynamics: new issues in classification. Biol Cybern **72**:447–453.